

AperTO - Archivio Istituzionale Open Access dell'Università di Torino

**Photochemical transformation of atrazine and formation of photointermediates under conditions relevant to sunlit surface waters: Laboratory**

**This is the author's manuscript**

*Original Citation:*

*Availability:*

This version is available <http://hdl.handle.net/2318/141263> since 2016-10-10T12:52:36Z

*Published version:*

DOI:10.1016/j.watres.2013.07.038

*Terms of use:*

Open Access

Anyone can freely access the full text of works made available as "Open Access". Works made available under a Creative Commons license can be used according to the terms and conditions of said license. Use of all other works requires consent of the right holder (author or publisher) if not exempted from copyright protection by the applicable law.

(Article begins on next page)



## UNIVERSITÀ DEGLI STUDI DI TORINO

This Accepted Author Manuscript (AAM) is copyrighted and published by Elsevier. It is posted here by agreement between Elsevier and the University of Turin. Changes resulting from the publishing process - such as editing, corrections, structural formatting, and other quality control mechanisms - may not be reflected in this version of the text. The definitive version of the text was subsequently published in

G. Marchetti, M. Minella, V. Maurino, C. Minero, D. Vione. Photochemical transformation of atrazine and formation of photointermediates under conditions relevant to sunlit surface waters: Laboratory measures and modelling. *Wat. Res.* **2013**, *47*, 6211-6222.  
DOI: 10.1016/j.waters.2013.07.038.

You may download, copy and otherwise use the AAM for non-commercial purposes provided that your license is limited by the following restrictions:

- (1) You may use this AAM for non-commercial purposes only under the terms of the CC-BY-NC-ND license.
- (2) The integrity of the work and identification of the author, copyright owner, and publisher must be preserved in any copy.
- (3) You must attribute this AAM in the following format:

G. Marchetti, M. Minella, V. Maurino, C. Minero, D. Vione. Photochemical transformation of atrazine and formation of photointermediates under conditions relevant to sunlit surface waters: Laboratory measures and modelling. *Wat. Res.* **2013**, *47*, 6211-6222.  
DOI: 10.1016/j.waters.2013.07.038 (<http://www.elsevier.com/locate/watres>).

# Photochemical transformation of atrazine and formation of photointermediates under conditions relevant to sunlit surface waters: Laboratory measures and modelling

Giulia Marchetti,<sup>a,b</sup> Marco Minella,<sup>a</sup> Valter Maurino,<sup>a</sup> Claudio Minero,<sup>a</sup> and Davide Vione<sup>a,c\*</sup>

<sup>a</sup> *Università degli Studi di Torino, Dipartimento di Chimica, Via P. Giuria 5, 10125 Torino, Italy. <http://www.chimicadellambiente.unito.it>*

<sup>b</sup> *LAV s.r.l., Strada Carignano 58/14, 10024 Moncalieri (TO), Italy. <http://www.lavsrl.it>*

<sup>c</sup> *Università degli Studi di Torino, Centro Interdipartimentale NatRisk, Via Leonardo da Vinci 44, 10095 Grugliasco (TO), Italy. <http://www.natrisk.org>*

\* Corresponding author. Tel. +39-011-6705296. Fax +39-011-6707615. [davide.vione@unito.it](mailto:davide.vione@unito.it)

## Abstract

By combination of laboratory experiments and modelling, we show here that the main photochemical pathways leading to the transformation of atrazine (ATZ, 2-chloro-4-ethylamino-6-isopropylamino-1,3,5-triazine) in surface waters would be direct photolysis, reaction with  $\bullet\text{OH}$  and with the triplet states of chromophoric dissolved organic matter ( ${}^3\text{CDOM}^*$ ). Reaction with  ${}^3\text{CDOM}^*$  would be favoured by elevated water depth and dissolved organic carbon content, while opposite conditions would favour direct photolysis and  $\bullet\text{OH}$  reaction. Desethylatrazine (DEA, 4-amino-2-chloro-6-isopropylamino-1,3,5-triazine) was the main detected intermediate of ATZ phototransformation. Its formation yield from ATZ (ratio of DEA formation to ATZ transformation rate) would be  $0.93\pm 0.14$  for  $\bullet\text{OH}$ ,  $0.55\pm 0.05$  for  ${}^3\text{CDOM}^*$ , and  $0.20\pm 0.02$  for direct photolysis. Direct photolysis and  $\bullet\text{OH}$  reaction also yielded 4-amino-2-hydroxy-6-isopropylamino-1,3,5-triazine (DEAOH) and 6-amino-2-chloro-4-ethylamino-1,3,5-triazine (DIA). Reaction with excited triplet states also produced 2-hydroxy-4,6-diamino-1,3,5-triazine (AN) and 2-chloro-4,6-diamino-1,3,5-triazine (CAAT). Therefore, if biological processes can be neglected and if the low formation yields do not prevent detection, DEAOH and DIA could be used as markers of ATZ direct photolysis and  $\bullet\text{OH}$  reaction, while AN and CAAT could be markers of ATZ reaction with  ${}^3\text{CDOM}^*$ . Model predictions concerning ATZ phototransformation were compared with available field data from the literature. When sufficiently detailed field information was provided, good agreement was found with the model.

**Keywords:** Environmental modelling; Surface-water photochemistry; Indirect photolysis; Photosensitisers; Pesticides; Atrazine.

## 1. Introduction

Atrazine (ATZ) is a triazine herbicide that is mainly intended to control broadleaf and some grassy weeds. For this reason it is extensively used in agricultural applications to corn and rice, but substantial use is also made in the case of sorghum and sugarcane. Moreover, ATZ is widely applied on non-agricultural sites such as lawns and turf. As far as the mode of action is concerned, ATZ blocks electron transport in chloroplast's photosystem II complex, thereby preventing CO<sub>2</sub> fixation and subsequent energy production. Plant death occurs mostly by desiccation following membrane damage, because of formation of reactive species (<sup>1</sup>O<sub>2</sub> and triplet-state chlorophyll) that trigger a chain reaction of lipid peroxidation (Brassard et al., 2003).

The quite high water solubility of ATZ (33 mg L<sup>-1</sup>; Mudhoo and Garg, 2011) favours the occurrence of this compound in surface and ground water, where it often exceeds the 10 µg L<sup>-1</sup> level of concern for aquatic ecosystems (USEPA, 2012). ATZ is moderately to slightly toxic to many fish species, and somewhat less toxic to aquatic invertebrates (Brassard et al., 2003; USEPA, 2012). Due to its intended use as an herbicide, ATZ is understandably highly toxic to aquatic vascular plants and algae (USEPA, 2012). As far as human health is concerned, the main risk related to ATZ exposure is connected to its endocrine-disruption capabilities (USEPA, 2012; Forgacs et al., 2012).

Although presently forbidden in the European Union, ATZ is still detected in EU countries (Silva et al., 2012; Bono-Blay et al., 2012), probably because of persistence in groundwater that may act as source for surface water and soil. Moreover, some illegal ATZ use cannot be excluded. More importantly, ATZ is extensively applied worldwide in both developed and developing countries (Bhullar et al., 2012; Reilly et al., 2012; Wang et al., 2012; Zhang et al., 2012).

Biotransformation and phototransformation are the main known pathways of ATZ removal from the environment. They produce a number of transformation intermediates such as desethylatrazine (DEA), desisopropylatrazine (DIA), chlorodiaminotriazine (CAAT), ammeline (AN), hydroxyatrazine (ATOH) and cyanuric acid (CYA) (Torrents et al., 1997; Larson et al., 2004; Mudhoo and Garg, 2011; see Table 1 for the structure of the cited compounds). Among photochemical pathways, direct photolysis and <sup>•</sup>OH reaction have received most attention to date (Torrents et al., 1997; Acero et al., 2000; Balci et al., 2009).

A proper modelling of pollutant photochemical fate in surface waters requires a quantitative assessment of additional pathways, such as reaction with CO<sub>3</sub><sup>•-</sup>, <sup>1</sup>O<sub>2</sub> and most notably the triplet states of chromophoric dissolved organic matter (<sup>3</sup>CDOM\*) (Latch et al., 2003; Canonica et al., 2005; Canonica et al., 2006; Halladja et al., 2007). Humic acids (HAs) have been shown to enhance or inhibit ATZ phototransformation (Minero et al., 1992; Prosen and Zupančič-Kralj, 2005; Garbin et al., 2007; Ou et al., 2009; Sun et al., 2011). This may happen because HAs compete with ATZ for irradiance, thereby inhibiting direct photolysis, and scavenge photogenerated transients such as <sup>•</sup>OH. However, HAs might also photosensitise ATZ degradation through the reaction of their triplet states (Hartenbach et al., 2008). Quantitative reactivity data are needed to assess the actual

environmental importance of ATZ transformation by natural sensitizers. Moreover, formation yields are required to model the photochemical production of transformation intermediates under environmental conditions (De Laurentiis et al., 2012). In the case of ATZ, such a task can be greatly favoured by the commercial availability of many known or potential phototransformation intermediates, which allows easy measurement of formation yields.

The present work has the purpose of modelling the photochemical fate of ATZ in surface waters. Reaction kinetic parameters were experimentally determined together with yields of major intermediates, which are formed *via* the main pathways of ATZ photoinduced transformation. The goal was to identify conditions that would favour or hamper ATZ phototransformation and intermediate formation, as well as to compare model predictions with field data.

## 2. Experimental

**2.1. Reagents and materials.** Atrazine (2-chloro-4-ethylamino-6-isopropylamino-1,3,5-triazine, ATZ), 2-chloro-4,6-diamino-1,3,5-triazine (CAAT), 2-hydroxy-4,6-diamino-1,3,5-triazine (ammeline, AN), 6-amino-4-ethylamino-2-hydroxy-1,3,5-triazine (DIAOH), 4-amino-2-hydroxy-6-isopropylamino-1,3,5-triazine (DEAOH), 6-amino-2-chloro-4-ethylamino-1,3,5-triazine (DIA), 4-amino-2-chloro-6-isopropylamino-1,3,5-triazine (DEA) and 4-ethylamino-2-hydroxy-6-isopropylamino-1,3,5-triazine (ATOH) were all Pestanal grade from Aldrich. Cyanuric acid (2,4,6-trihydroxy-1,3,5-triazine, CYA, purity grade 98%), anthraquinone-2-sulphonic acid sodium salt (AQ2S, 97%), sodium hexanesulphonate (> 99%) and H<sub>3</sub>PO<sub>4</sub> (85%) were purchased from Aldrich, H<sub>2</sub>O<sub>2</sub> (30%), NaNO<sub>3</sub> (>99.5%) and NaHCO<sub>3</sub> (99%) from VWR Int., methanol (gradient grade) from Carlo Erba (Rodano, Italy), Rose Bengal from Alfa Aesar. Water used was of Milli-Q quality.

**2.2. Irradiation experiments.** Irradiation experiments were carried out on synthetic solutions prepared by dissolving the relevant compounds in Milli-Q water. The stock ATZ solution (0.1 mM) was prepared by dissolving the solid in water, without use of organic solvents that could introduce a bias in irradiation experiments in the presence of photoreactive transients. Solutions to be irradiated (5 mL volume) were placed inside cylindrical Pyrex glass cells (4.0 cm diameter, 2.5 cm height) having a lateral neck tightly closed with a screw cap. Cells were magnetically stirred during illumination, which took place mainly from the top. The direct photolysis of 20 μM ATZ was studied upon ultraviolet-B (UVB, 290-320 nm) irradiation under a 20 W Philips TL 01 RS lamp (emission maximum at 313 nm). The incident irradiance over the solutions was 9.8±0.2 W m<sup>-2</sup> between 290 and 400 nm, measured with a CO.FO.ME.GRA. (Milan, Italy) power meter. The incident photon flux into irradiated solutions was (6.4±0.1)·10<sup>-6</sup> Einstein L<sup>-1</sup> s<sup>-1</sup>. It was actinometrically determined using the ferrioxalate method (Kuhn et al., 2004), taking into account the wavelength-dependent quantum yield of Fe<sup>2+</sup> photoproduction. Note that ferrioxalate has considerable radiation absorption in the UVB, where ATZ mostly absorbs environmentally-

significant radiation. Figure 1a reports the spectrum of incident radiation into the solutions (spectral photon flux density), measured with an Ocean Optics SD2000 CCD spectrophotometer (calibrated with an Ocean Optics DH-2000-CAL source), taking into account Pyrex transmittance and normalising to actinometry data. The Figure also reports the absorption spectrum of ATZ (molar absorption coefficient), taken with a Varian CARY 100 Scan double-beam UV-Vis spectrophotometer, using quartz cuvettes with 10 mm path length. The choice of the lamp to study direct photolysis is appropriate, due to the fact that the limited absorption of sunlight by ATZ mainly takes place in the UVB region (for instance, it is  $\epsilon_{ATZ}^{300nm} \sim 300 \text{ M}^{-1} \text{ cm}^{-1}$  and  $\epsilon_{ATZ}^{320nm} \sim 100 \text{ M}^{-1} \text{ cm}^{-1}$ ). Moreover, UVB absorption by ATZ represents the tail of an absorption band with maximum at 260-270 nm (the latter wavelengths belonging to the UVC region). Because only one band is involved in UVB absorption, the photolysis quantum yield is expected not to vary significantly with wavelength (Warneck and Wurzinger, 1988; Fischer and Warneck, 1996).

Reaction between ATZ and  $\bullet\text{OH}$  was studied upon irradiation of 1 mM  $\text{H}_2\text{O}_2$  under a 20 W Philips TL 09N lamp, with emission maximum at 351 nm,  $58.6 \pm 1.4 \text{ W m}^{-2}$  incident irradiance (290 - 400 nm), and  $(4.4 \pm 0.1) \cdot 10^{-5} \text{ Einstein L}^{-1} \text{ s}^{-1}$  incident photon flux. The same lamp was used to study reaction between ATZ and  $\text{CO}_3^{\bullet-}$ , irradiating 1 mM  $\text{NaNO}_3 + \text{NaHCO}_3$  (the latter up to 10 mM). Figure 1b reports the incident spectral photon flux density of the TL 09N lamp and the molar absorption coefficients of  $\text{H}_2\text{O}_2$  and  $\text{NO}_3^-$ . Note that ATZ absorbs radiation emitted by the TL 09N lamp, thus some direct photolysis of ATZ under such conditions is expected (although minor, *vide infra*).

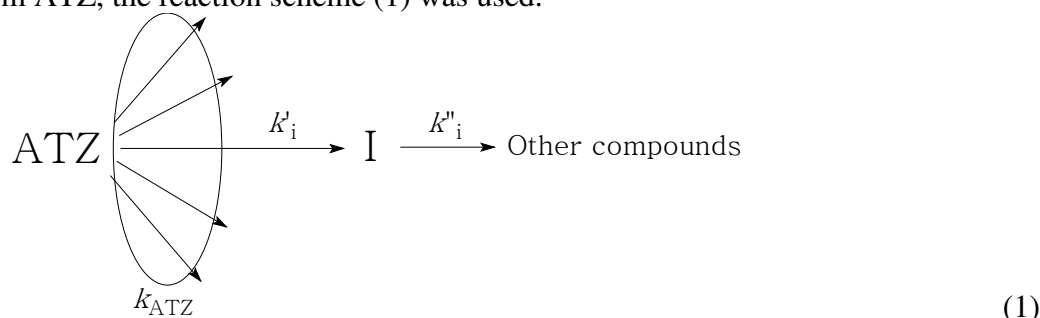
AQ2S was used as CDOM proxy, to study the reactivity between ATZ and  ${}^3\text{CDOM}^*$ , because no estimate of the relevant reaction rate constant is available in the literature. Reasons for the choice of AQ2S are the high abundance of quinones in CDOM (Cory and McKnight, 2005) and the fact that  ${}^3\text{AQ2S}^*$  does not yield interfering species such as  ${}^1\text{O}_2$  and  $\bullet\text{OH}$  (Loeff et al., 1983; Maddigapu et al., 2010), unlike other triplet sensitizers. To achieve selective excitation of AQ2S, solutions were irradiated under a Philips TLK 03 lamp, with emission maximum at 436 nm and  $(1.0 \pm 0.2) \cdot 10^{-4} \text{ Einstein L}^{-1} \text{ s}^{-1}$  incident photon flux. Figure 1c reports the spectral photon flux density of incident radiation and the molar absorption coefficient of AQ2S. The initial AQ2S concentration was 0.1 mM, to avoid the additional complication caused by reaction between excited and ground-state AQ2S at higher concentration values (Bedini et al., 2012).

With the exception of the nitrate + bicarbonate system, the pH of irradiated solutions was around 6 (natural pH). Very limited pH variations (within 0.5 units) were observed upon ATZ irradiation under the different conditions.

**2.3. Analytical determinations.** After irradiation, solutions were analysed by high-performance liquid chromatography coupled with diode array detection (HPLC-DAD). The adopted LaChrom Elite instrument (VWR-Hitachi) was equipped with L-2200 Autosampler (injection volume 60  $\mu\text{L}$ ), L-2130 quaternary pump for low-pressure gradients, L-2300 column oven (set at 40°C), and L-2455 DAD detector. The column used was a RP-C18 LichroCART (VWR Int., length 125 mm, diameter

4 mm), packed with LiChrospher 100 RP-18 (5  $\mu\text{m}$  diameter). To determine ATZ and its possible transformation intermediates, elution was carried out with the following gradient (flow rate 1.0 mL  $\text{min}^{-1}$ ), where A is methanol and B an aqueous solution containing 10 mM sodium hexanesulphonate, 14 mM  $\text{H}_3\text{PO}_4$  and 0.5% methanol: 100%B for 4 min, then linearly down to 30% B reached at 20 min, back in 2 min to the initial conditions that were kept for a further 8 min. Chromatographic retention times are shown in Table 1, which also reports the structural formulae of the monitored compounds as well as their names and acronyms. Though DEAOH and DIA were found to co-elute, it was possible to quantify their concentrations by exploiting the fact that DIA absorbs radiation at 260 nm where DEAOH does not absorb significantly. Considering that the DIA peak area at 220 nm is 8.7 times higher than at 260 nm, by monitoring DIA at 260 nm it was possible to achieve its direct quantification and to assess its expected contribution to the co-elution peak at 220 nm. Therefore, the amount of DEAOH was determined by difference. This procedure was made easier and reasonably accurate by the fact that DIA and DEAOH reached comparable concentration values in the studied samples.

**2.4. Kinetic data treatment.** The experimental time trends of ATZ were fitted with pseudo-first order equations  $C_t = C_o \cdot e^{-k_{\text{ATZ}} t}$ , where  $C_t$  is ATZ concentration at the time  $t$ ,  $C_o$  its initial concentration and  $k_{\text{ATZ}}$  the transformation rate constant. For the time evolution of the intermediate I from ATZ, the reaction scheme (1) was used.



$$\frac{dC_t}{dt} = -k_{\text{ATZ}} C_t \quad (2)$$

$$\frac{dI_t}{dt} = k_i' C_t - k_i'' I_t \quad (3)$$

The rate constants reported on the reaction arrows of (1) are pseudo-first order ones, from which the system of differential equations (2,3) can be obtained. The solution of the system yielded the equation  $I_t = k_i' C_o (k_i'' - k_{\text{ATZ}})^{-1} (e^{-k_{\text{ATZ}} t} - e^{-k_i'' t})$ , where  $C_o$  and  $k_{\text{ATZ}}$  are as above,  $I_t$  is the concentration of intermediate  $i$  at the time  $t$ ,  $k_i'$  the first-order rate constant of  $i$  formation from ATZ, and  $k_i''$  the first-order rate constant of  $i$  transformation. The initial rate of ATZ disappearance is  $R_{\text{ATZ}} = k_{\text{ATZ}} C_o$ , that of  $i$  formation is  $R_i' = k_i' C_o$ . Errors on rates ( $\pm\sigma$ ) were derived from scattering of experimental data around the fit curves. Reproducibility of repeated runs was in the range of 10-15%.

**2.5. Photochemical model.** The model used in this work to assess the environmental photochemistry of ATZ and of its intermediates has been previously described (Vione et al., 2010a; Maddigapu et al., 2011; Minella et al., 2011; Sur et al., 2012). Briefly, it predicts steady-state concentrations of  $\bullet\text{OH}$ ,  $\text{CO}_3^{\bullet-}$ ,  $^1\text{O}_2$  and  $^3\text{CDOM}^*$  based on water chemical composition and depth and on the spectral photon flux density of sunlight. The model also predicts reaction kinetics (pseudo-first order rate constants) of pollutants with  $\bullet\text{OH}$ ,  $\text{CO}_3^{\bullet-}$ ,  $^1\text{O}_2$  and  $^3\text{CDOM}^*$ , as well as kinetics of direct photolysis. Required input data are photolysis quantum yield and second-order reaction rate constants with  $\bullet\text{OH}$ ,  $\text{CO}_3^{\bullet-}$ ,  $^1\text{O}_2$  and  $^3\text{CDOM}^*$ . Formation yields of intermediates *via* the different photochemical pathways are required to model the formation rate constants. The standardised time unit used by the model is a summer sunny day (SSD), equivalent to fair-weather 15 July at 45°N latitude (Vione et al., 2011). By so doing, it is possible to take into account the day-night cycle and to use a time unit that is related to outdoor conditions but that has definite duration. Obviously, photochemical reaction kinetics would be slower with cloudy weather or in other seasons than summer (Tixier et al., 2003). Further details including model equations are given elsewhere (Maddigapu et al., 2011; Sur et al., 2012; De Laurentiis et al., 2012).

One of us (DV) has recently derived a software application from the model (APEX: Aqueous Photochemistry of Environmentally-occurring Xenobiotics), which is available for free download at <http://chimica.campusnet.unito.it/do/didattica.pl/Quest?corso=7a3d> (including the User's Guide that contains a comprehensive account of model equations).

### 3. Results and Discussion

#### 3.1. ATZ phototransformation kinetics

To model ATZ photochemistry in surface waters, reactivity data are needed *via* the main photochemical reaction pathways (quantum yield of direct photolysis and reaction rate constants with  $\bullet\text{OH}$ ,  $\text{CO}_3^{\bullet-}$ ,  $^1\text{O}_2$  and  $^3\text{CDOM}^*$ ). Reasonably agreeing values of the reaction rate constant between ATZ and  $\bullet\text{OH}$  are available in the literature ( $3 \cdot 10^9 \text{ M}^{-1} \text{ s}^{-1}$ : Acero et al., 2000;  $2.4 \cdot 10^9 \text{ M}^{-1} \text{ s}^{-1}$ : Balci et al., 2009), from which a reasonable average  $k_{\text{ATZ}, \bullet\text{OH}} = (2.7 \pm 0.3) \cdot 10^9 \text{ M}^{-1} \text{ s}^{-1}$  can be obtained. Other quantities, including the photolysis quantum yield under steady irradiation were determined in this work, following an experimental protocol that is described in detail elsewhere (De Laurentiis et al., 2012; Sur et al., 2012). A screening method using nitrate UVB photolysis in the presence of bicarbonate was employed to test reactivity with  $\text{CO}_3^{\bullet-}$  (Vione et al., 2009), and the results suggested that reaction between ATZ and  $\text{CO}_3^{\bullet-}$  would not be very important in environmental waters (see SM). Huang and Mabury (2000) found a reaction rate constant between ATZ and  $\text{CO}_3^{\bullet-}$  of  $4 \cdot 10^6 \text{ M}^{-1} \text{ s}^{-1}$  which, given the typical concentration values of  $\bullet\text{OH}$  and  $\text{CO}_3^{\bullet-}$  in surface waters, means that the importance of reaction between ATZ and  $\text{CO}_3^{\bullet-}$  would be  $\leq 10\%$  of that with  $\bullet\text{OH}$ . This is comparable to the experimental uncertainty on the  $\bullet\text{OH}$  rate constant and it is lower than the model uncertainty on  $[\bullet\text{OH}]$ , which suggests a secondary role of  $\text{CO}_3^{\bullet-}$  in ATZ



phototransformation in surface waters. Rose Bengal was used as  $^1\text{O}_2$  source, and AQ2S as CDOM proxy. The results of these experiments and the calculations to determine the relevant rate constants are reported as Supplementary Material (hereafter SM). Results are listed in Table 2 as photolysis quantum yield  $\Phi_{\text{ATZ}}$  and second-order reaction rate constants between ATZ and reactive transients.

An interesting issue is that the quantum yield of ATZ photolysis in the UVB region is of the same order of magnitude as (but lower than) the 254 nm photolysis quantum yield (0.03; Bolton and Stefan, 2002; Prosen and Zupančič-Kralj, 2005). It should be considered that absorption bands at lower wavelengths are usually involved into more energetic photochemical processes, with higher photolysis quantum yields compared to bands at higher wavelengths (Fischer and Warneck, 1996). In the case of ATZ, absorbance at 254 nm has contribution from two bands (see Figure 1a), one with absorption maximum at  $\sim 220$  nm and the other with maximum at  $\sim 265$  nm. In contrast, UVB absorption of ATZ is only accounted for by the higher-wavelength band. Therefore, it is not surprising to find lower photolysis quantum yield of ATZ in the UVB (280-320 nm) compared to the UVC region ( $<280$  nm).

### 3.2. Formation of intermediates

Figure 2 reports the time evolution of 20  $\mu\text{M}$  ATZ and of its detected intermediates (DEA, DEAOH and DIA) upon UVB irradiation of ATZ (direct photolysis). The three intermediates reached comparable concentration values, although DEA was formed in highest amount. All other compounds listed in Table 1 were monitored, but their concentration values were below detection limit. The reported data allow intermediate formation yields to be determined. Assume  $i$  as a generic transformation intermediate of ATZ, with initial formation rate  $R'_i$ , and  $R_{\text{ATZ}}$  as the initial transformation rate of ATZ (see previous section 2.4 for the calculation of  $R'_i$  and  $R_{\text{ATZ}}$ ). The formation yield of  $i$  from ATZ is  $\eta_i = R'_i(R_{\text{ATZ}})^{-1}$ , where in the case of direct photolysis  $i = \text{DEA}$ , DEAOH, DIA. The yield values thus calculated for the three intermediates are reported in Table 2. It can be seen from the Table data that the detected intermediates account for approximately 40% of ATZ transformation, which means that an important fraction of the substrate is transformed into undetected compounds.

Figure 3 reports the time trends of ATZ (20  $\mu\text{M}$  initial concentration), DEA, DEAOH and DIA upon irradiation of 1 mM  $\text{H}_2\text{O}_2$  as  $\bullet\text{OH}$  source. Other compounds were below detection limit. Note that the same intermediates (but with different yields) were detected upon direct photolysis and  $\bullet\text{OH}$  reaction. Interestingly, a similar behaviour has been reported for the anti-epileptic drug carbamazepine (De Laurentiis et al., 2012). Considering the overlap between  $\text{H}_2\text{O}_2$  and ATZ absorption spectra (see Figure 1), ATZ excitation could not be avoided. However, ATZ direct photodegradation was tested under the TL 09N lamp adopted to excite  $\text{H}_2\text{O}_2$ , and the time scales of direct photolysis and  $\bullet\text{OH}$  reaction were found to be very different (7 days vs. 4 hours, respectively). The degradation rate of ATZ was  $\sim 25$  times higher in the presence of  $\text{H}_2\text{O}_2$  than in its absence, which would ensure a negligible interference of direct photolysis over  $\bullet\text{OH}$ -induced processes. As a

further check, addition of the  $\bullet\text{OH}$  scavenger 2-propanol (Buxton et al., 1988) in the 0.3-3 mM range was able to quench intermediate formation upon  $\text{H}_2\text{O}_2$  irradiation, at least over an irradiation time of 4 h. Higher concentration values of 2-propanol were not tested, because alcohols at high concentration might interfere with direct photolysis processes if they proceed through triplet states (Vione et al., 2010b). The above arguments suggest that the formation of DEA, DEAOH and DIA upon irradiation of 1 mM  $\text{H}_2\text{O}_2$  would be mostly accounted for by  $\bullet\text{OH}$ . Interestingly, under  $\bullet\text{OH}$  reaction conditions the concentration values as well as the initial formation rate of DEA were an order of magnitude higher compared to DIA and DEAOH, which is reflected by the relevant formation yields (Table 2). The high observed DEA yield is in reasonable agreement with Torrents et al. (1997), who report DEA as the main intermediate of ATZ transformation upon nitrate photolysis ( $\bullet\text{OH}$  source). The data of Table 2 suggest that DEA, DEAOH and DIA would account for about the totality of ATZ transformation by  $\bullet\text{OH}$ . A tentative scheme of the possible chain-shortening pathway leading from ATZ to DEA in the presence of  $\bullet\text{OH}$  is provided in SM (Scheme SMi).

Figure 4a reports the time trend of DEA formation upon irradiation of ATZ with 0.1 mM AQ2S, for different values of initial ATZ. With increasing ATZ one observes higher formation of DEA, which was the main intermediate also in this case. The other quantified intermediates were AN and CAAT (Figure 5). These compounds were above detection limit only at the highest adopted ATZ concentrations. ATOH and CYA were also tentatively detected, but ATOH was around detection limit and CYA was affected by chromatographic interference, possibly arising from AQ2S transformation intermediates. Formation with AQ2S of AN and CAAT instead of DEAOH and DIA suggests that the two pairs of compounds could be markers of triplet-sensitised processes and of  $\bullet\text{OH}$  reaction and direct photolysis, respectively. Table 2 reports the yields of AN and CAAT, calculated from the initial rates ( $\eta_i = R'_i(R_{ATZ})^{-1}$ , as discussed above), in the presence of 20  $\mu\text{M}$  initial ATZ. The concentration of CAAT formed from 15  $\mu\text{M}$  ATZ was quite near the quantification limit and it might be inaccurate, thus the CAAT formation yield was determined only for 20  $\mu\text{M}$  initial ATZ. Application of the same procedure to the DEA yield gave a value affected by large uncertainty ( $\eta_{DEA}^{3AQ2S^*} = 0.57 \pm 0.22$ ). However, an alternative procedure was enabled by detection of DEA in the presence of several initial concentration values of ATZ. With irradiated AQ2S, the trend of ATZ initial transformation rate ( $R_{ATZ}$ ) as a function of ATZ concentration was linear below 10  $\mu\text{M}$  ATZ (Figure SM5), as  $R_{ATZ} = (1.00 \pm 0.05) \cdot 10^{-4} [\text{ATZ}]$ . A linear trend was also obtained for DEA initial formation rate versus ATZ initial concentration ( $\leq 10 \mu\text{M}$ ), as shown in Figure 4b. Linear fit of experimental data gave  $R'_{DEA} = (5.5 \pm 0.2) \cdot 10^{-5} [\text{ATZ}]$ , from which one obtains  $\eta_{DEA}^{3AQ2S^*} = R'_{DEA} (R_{ATZ})^{-1} = 0.55 \pm 0.05$ . This result is fully compatible with that obtained with 20  $\mu\text{M}$  ATZ, but it has considerably lower uncertainty. Therefore, it is reported in Table 2 and it is used hereafter as representative of the DEA yield with  $^3\text{CDOM}^*$ . Finally, note that DEA, AN and CAAT would account for about 60% of ATZ transformation, while the remainder would consist of undetected compounds.

Photoreactivity measures reported in the SM suggest that ATZ would undergo minor to negligible reaction with  $\text{CO}_3^{\bullet-}$  and  $^1\text{O}_2$ . In the latter case, practically no degradation was observed upon irradiation of ATZ in the presence of Rose Bengal over a time scale of 16-24 h. DEA was only detected at trace levels at the highest adopted ATZ concentration (20  $\mu\text{M}$ ). For  $\text{CO}_3^{\bullet-}$ , irradiation of both 1 mM  $\text{NaNO}_3$  + 10 mM  $\text{NaHCO}_3$  (used to produce  $\text{CO}_3^{\bullet-}$ ) and of 1 mM  $\text{NaNO}_3$  alone (used to produce  $\bullet\text{OH}$ ) at the same pH (8.2 by phosphate buffer) produced the same intermediates (DEA, DEAOH, DIA, CAAT). However, initial formation rates were lower in the case of  $\text{NaNO}_3$  +  $\text{NaHCO}_3$  compared to  $\text{NaNO}_3$  alone, because of  $\bullet\text{OH}$  scavenging carried out by bicarbonate to produce  $\text{CO}_3^{\bullet-}$  (Buxton et al., 1988). Therefore, there is no evidence that DEA, DEAOH, DIA and CAAT would be formed from  $\text{ATZ} + \text{CO}_3^{\bullet-}$ , because they could also be produced by species generated upon nitrate photolysis ( $\bullet\text{OH}$  and  $\bullet\text{NO}_2$ ). Moreover, the secondary environmental importance of reaction between ATZ and  $\text{CO}_3^{\bullet-}$  suggests that the associated intermediate yields can be safely neglected.

### 3.3. Photochemical modelling

The data reported in Table 2 allow the modelling, as a function of water chemical composition and column depth, of (i) half-life times and transformation rate constants of ATZ, and (ii) formation rate constants and yields of intermediates. Chemical parameters of photochemical importance are nitrate ( $\bullet\text{OH}$  source), nitrite (important  $\bullet\text{OH}$  source and minor sink), carbonate and bicarbonate ( $\bullet\text{OH}$  sinks and  $\text{CO}_3^{\bullet-}$  sources) and dissolved organic matter (DOM), measured as DOC (Dissolved Organic Carbon) or NPOC (Non-Purgeable Organic Carbon). DOM is a major  $\bullet\text{OH}$  sink and, as far as its chromophoric fraction CDOM is concerned, a source of  $^3\text{CDOM}^*$ ,  $^1\text{O}_2$  and  $\bullet\text{OH}$  (Maddigapu et al., 2011; Sur et al., 2012).

#### 3.3.1. ATZ phototransformation kinetics

Preliminary photochemical modelling indicated that direct photolysis and reaction with  $\bullet\text{OH}$  and  $^3\text{CDOM}^*$  would be the main ATZ phototransformation pathways. The relative importance of the three processes depends on environmental conditions: for instance, with 50  $\mu\text{M}$  nitrate, 1  $\mu\text{M}$  nitrite, 2 mM bicarbonate, 10  $\mu\text{M}$  carbonate, 1 mg C  $\text{L}^{-1}$  DOC and a depth of 5 m (reasonable conditions in the water of a shallow lake),  $\bullet\text{OH}$  would account for  $24\pm 6\%$  of ATZ transformation,  $^3\text{CDOM}^*$  for  $23\pm 9\%$ , and direct photolysis for  $53\pm 11\%$ . With greater DOC (5 mg C  $\text{L}^{-1}$ ) and other conditions as above, the percentages would be  $8\pm 2\%$  for  $\bullet\text{OH}$ ,  $76\pm 29\%$  for  $^3\text{CDOM}^*$ , and  $16\pm 3\%$  for direct photolysis. Note that  $\text{CO}_3^{\bullet-}$  would always account for  $<5\%$  of ATZ phototransformation, and reaction with  $^1\text{O}_2$  would be completely negligible.

Reaction with  $\bullet\text{OH}$  and direct photolysis would prevail in shallow and DOM-poor water bodies, while opposite conditions would favour  $^3\text{CDOM}^*$ . Indeed, DOM-rich water usually contains elevated CDOM that absorbs visible radiation in addition to the UV one. Visible light can reach deeper water layers compared to UV radiation, which explains why CDOM-induced processes tend

to prevail in deeper water bodies. Nitrate and nitrite as  $\bullet\text{OH}$  sources would understandably favour  $\bullet\text{OH}$  reactions. This happens despite the fact that nitrite also consumes  $\bullet\text{OH}$  (Buxton et al., 1988), because the role of nitrite as  $\bullet\text{OH}$  scavenger is very minor compared to DOM. In contrast, the role of nitrite as  $\bullet\text{OH}$  source is on average lower compared to CDOM, but it is of almost comparable importance (Takeda et al., 2004).

Figure 6 reports the modelled half-life time  $t_{1/2}$  (6a) and the pseudo-first order degradation rate constant  $k$  (6b) of ATZ, as a function of nitrite and DOC. Other assumed conditions are 5 m water depth, 50  $\mu\text{M}$  nitrate, 2 mM bicarbonate and 10  $\mu\text{M}$  carbonate. The trends of  $t_{1/2}$  and  $k$  are opposite, because  $t_{1/2} = (\ln 2) k^{-1}$ . There is a small enhancement of ATZ phototransformation with increasing nitrite (of about 5-10%), in particular at low organic matter (DOC), in which conditions nitrite is an important  $\bullet\text{OH}$  source compared to CDOM. The figure also shows that ATZ degradation gets slower with increasing DOC. CDOM is a source of  $\bullet\text{OH}$  and  ${}^3\text{CDOM}^*$ , but it also competes with ATZ for irradiance, thereby inhibiting the direct photolysis. Furthermore, DOM as  $\bullet\text{OH}$  scavenger quenches the corresponding process of ATZ transformation.

### 3.3.2. Intermediate formation kinetics

Figure 7a reports the pseudo-first order rate constant of DEA formation from ATZ,  $(k_{\text{DEA}})'$ . The rate constant is somewhat enhanced by nitrite (particularly at low DOC), and inhibited by (C)DOM, which inhibits both  $\bullet\text{OH}$  reaction and direct photolysis. Such effects would not be compensated for by the enhancement of  ${}^3\text{CDOM}^*$  with increasing DOC, as already shown for ATZ transformation (Figure 6a). The formation rate constants of DIA and DEAOH (data not shown) have similar trends as for DEA, but they have lower absolute values because of lower formation yields (see Table 2). Moreover, DIA and DEAOH are not formed upon reaction between ATZ and  ${}^3\text{CDOM}^*$ , thus their formation rate constants undergo slightly faster decrease with increasing DOC compared to DEA.

Figure 7b reports the pseudo-first order formation rate constants of CAAT and AN  $((k_{\text{CAAT}})'$  and  $(k_{\text{AN}})'$ , respectively). They have equal values, because of equal formation yields from ATZ upon  ${}^3\text{CDOM}^*$  reaction (see Table 2) and negligible formation from other processes. Reactions involving  ${}^3\text{CDOM}^*$  would be enhanced at high DOC, which accounts for the increase of  $(k_{\text{CAAT}})'$  and  $(k_{\text{AN}})'$  with increasing content of organic matter. Because CAAT and AN are not expected to be formed from  $\text{ATZ} + \bullet\text{OH}$ , nitrite has no effect on their formation kinetics.

### 3.3.3. Intermediate formation yields

Formation yields of intermediates (Figure 8) are the ratios between their pseudo-first order formation rate constants and the transformation rate constant of ATZ. The general expression of the modelled yield of an intermediate  $i$  is  $\eta_i = (k_i)'(k_{tot}^{ATZ})^{-1} = (k_{tot}^{ATZ})^{-1} \sum_p (\eta_p^i k_p^{ATZ})$  (De Laurentiis et al., 2012), where  $p$  is a photochemical process (*e.g.* photolysis,  $\bullet\text{OH}$ ,  ${}^3\text{CDOM}^*$ ). The values of  $\eta_p^i$  (yield of  $i$  via the process  $p$ ) are reported in Table 2 and those of  $k_p^{ATZ}$  (degradation rate constant of ATZ via the process  $p$ ) are obtained from the model. It is also  $k_{tot}^{ATZ} = \sum_p k_p^{ATZ}$ . The formation yield  $\eta_i$  is increased by conditions that favour a process  $p$  with high  $\eta_p^i$ , and decreased if the prevailing process has low or nil  $\eta_p^i$ . Figure 8 reports the formation yields from ATZ of DEA (8a), DIA (8b) and CAAT, AN (8c). Note that  $\eta_{DEA\text{OH}}$  (data not shown) has similar values and same trend as  $\eta_{DIA}$ . The yields of CAAT and AN are the same, because  $\eta_{{}^3\text{CDOM}^*}^{\text{CAAT}} = \eta_{{}^3\text{CDOM}^*}^{\text{AN}}$  (Table 2) and  ${}^3\text{CDOM}^*$  is the only process that gives such compounds.

The DEA yield from ATZ is highest for  $\bullet\text{OH}$ , lowest for direct photolysis and it has an intermediate value in the case of  ${}^3\text{CDOM}^*$  (Table 2). Coherently, high values of  $\eta_{\text{DEA}}$  are observed at high nitrite (important  $\bullet\text{OH}$  source and very minor scavenger) and low DOC (DOM is an  $\bullet\text{OH}$  scavenger) (Figure 8a). If DOC is high, DOM efficiently consumes  $\bullet\text{OH}$ , CDOM inhibits ATZ photolysis by competing for sunlight irradiance, and ATZ degradation by  ${}^3\text{CDOM}^*$  is enhanced. For these reasons,  $\eta_{\text{DEA}}$  approaches the value  $\eta_{{}^3\text{CDOM}^*}^{\text{DEA}} = 0.55$  at high DOC. An interesting issue is the minimum of  $\eta_{\text{DEA}}$  vs. DOC. Reaction between ATZ and  ${}^3\text{CDOM}^*$  requires  $\text{DOC} > 1 \text{ mg C L}^{-1}$  to be important. Below or around  $1 \text{ mg C L}^{-1}$  DOC, the increase of DOC mainly increases the relative importance of direct photolysis vs.  $\bullet\text{OH}$ . In fact,  $\bullet\text{OH}$  scavenging by DOM is more effective than competition for irradiance between CDOM and ATZ. Replacement of  $\bullet\text{OH}$  reaction with photolysis decreases the DEA yield ( $\eta_{\text{Phot}}^{\text{DEA}} < \eta_{\text{OH}}^{\text{DEA}}$ , Table 2), and one can have  $\eta_{\text{DEA}} < \eta_{{}^3\text{CDOM}^*}^{\text{DEA}}$ . The increasing importance of  ${}^3\text{CDOM}^*$ , above  $1 \text{ mg C L}^{-1}$  DOC, accounts for the increase of  $\eta_{\text{DEA}}$  under such conditions, thereby producing the  $\eta_{\text{DEA}}$  minimum around  $1 \text{ mg C L}^{-1}$  DOC (Figure 8a).

Figure 8b reports the DIA yield from ATZ,  $\eta_{\text{DIA}}$ . The yield decreases with increasing DOC because of inhibition by organic matter (DOM and CDOM) of both  $\bullet\text{OH}$  reaction and direct photolysis. Moreover, DIA is not formed from  $\text{ATZ} + {}^3\text{CDOM}^*$ . Increasing nitrite enhances the  $\bullet\text{OH}$  process, but it has very little effect on  $\eta_{\text{DIA}}$ . Actually, ATZ direct photolysis and reaction with  $\bullet\text{OH}$  produce DIA with similar yields (see Table 2), and the fact that nitrite enhances  $\bullet\text{OH}$  reaction at the expense of direct photolysis has low effect on  $\eta_{\text{DIA}}$ . Figure 8c reports the yields of CAAT and AN. They are low (<2%, see the Figure), but they increase with increasing DOC. This is consistent with the fact that the two compounds are produced by  $\text{ATZ} + {}^3\text{CDOM}^*$ , because [ ${}^3\text{CDOM}^*$ ] increases with increasing DOC (see for instance Figure SM6). The slight decrease of the yields with increasing nitrite ( $\leq 5\%$ ) is due to the fact that reaction between ATZ and  $\bullet\text{OH}$  does not produce CAAT or AN.

Figures 7 and 8 suggest that DEA would always be the main intermediate of ATZ transformation. Moreover, increasing DOC would shift secondary intermediates from DIA and

DEAOH to CAAT and AN. It is not straightforward to use intermediate profiles to distinguish ATZ photochemical pathways in the environment, because of the large overlap of photo- and biotransformation compounds (Mudhoo and Garg, 2011). Literature evidence suggests that differentiation between biotic and abiotic transformation could possibly be carried out by compound-specific isotope analysis. Reaction with  $\bullet\text{OH}$  and  ${}^3\text{CDOM}^*$  enriches residual ATZ with  ${}^{13}\text{C}$ ,  ${}^2\text{H}$ , and  ${}^{15}\text{N}$  (Hartenbach et al., 2008), while biodegradation increases  ${}^{13}\text{C}$  and depletes  ${}^{15}\text{N}$  (Meyer et al., 2009). Detection of DIA & DEAOH vs. CAAT & AN, if allowed by the low formation yields of the latter, could give insight into photochemical pathways, but only under conditions where ATZ photodegradation strongly prevails over biotransformation.

### ***3.4. Comparison of model predictions with field data***

Despite the wide number of studies addressing the topic of ATZ occurrence and fate in surface waters, it is difficult to find field data that allow comparison with model predictions. Few studies report a half-life time or pseudo-first order rate constant that can be attributed to ATZ transformation, after taking into account other processes such as transport or phase partitioning. The transport issue is of considerable importance in the case of rivers and streams, where it is a key confounding factor. When transformation half-lives are available, photochemical modelling is often prevented by the lack of key data concerning water chemical composition and/or depth. Therefore, most available field studies could not be compared to our model predictions.

A field work that enabled straightforward comparison was carried out in the Patuxent river estuary, flowing into Chesapeake Bay, Maryland, USA (McConnell et al., 2004). ATZ half-life time was determined in two downstream sites, a shallow (1 m depth) and a deeper one (10 m). In both cases average DOC was around  $5 \text{ mg C L}^{-1}$  and, under such conditions (prevailing  ${}^3\text{CDOM}^*$  reaction according to our model), the predicted photochemical half-life time of ATZ would be poorly influenced by the concentration values of nitrate and nitrite ( $\bullet\text{OH}$  sources) or bicarbonate and carbonate ( $\bullet\text{OH}$  scavengers). The field study yielded half-life times of 20-21 and 67-100 days in the shallow and deep site, respectively. The authors supposed photochemistry to be important in the transformation of ATZ (McConnell et al., 2004). By comparison, upon application of our model to water chemistry data from Chesapeake Bay, with the ATZ reactivity parameters reported in Table 2, one obtains half-life times of  $17 \pm 4$  and of  $64 \pm 18$  days, respectively, in very good agreement with field data. Model errors ( $\pm\sigma$ ) were determined using the *APEX\_Errors.xls* function of the APEX software.

It can be hypothesised that photochemistry plays an important role in ATZ degradation in relatively shallow water bodies illuminated by sunlight. Low DOC values favour photochemical processes (see Figure 6a), but the presence of low DOC is not essential because reaction with  ${}^3\text{CDOM}^*$  would prevail over  $\bullet\text{OH}$  and direct photolysis in DOM-rich water.

Other field studies report that both photochemistry and biotransformation could play an important role in ATZ degradation (Kolpin and Kalkhoff, 1993; Chung and Gu, 2009).

Unfortunately, the incomplete water chemistry data provided in the relevant papers did not allow comparison between model predictions and field data.

#### 4. Conclusions

- The main pathways involved in ATZ phototransformation in surface waters would be direct photolysis and reactions with  $\bullet\text{OH}$  and  ${}^3\text{CDOM}^*$ .  $\bullet\text{OH}$  reactions and direct photolysis would be favoured in shallow, DOM-poor and (for  $\bullet\text{OH}$ ) nitrate- and nitrite-rich environments. Such circumstances would produce fastest ATZ phototransformation. Opposite conditions would enhance the relative role of  ${}^3\text{CDOM}^*$ , with slower photodegradation of ATZ. Good agreement between model predictions and field data could be obtained for ATZ transformation in the Patuxent river estuary (Maryland, USA), implying that ATZ photodegradation is important in that environment. Interestingly, estuaries can be very favourable sites for photochemical reactions (Al Housari et al., 2010; Maddigapu et al., 2011).
- DEA would be the main intermediate of ATZ transformation upon both direct and indirect photolysis. Its formation yield is very high upon  $\bullet\text{OH}$  reaction ( $0.93\pm 0.14$ ), and lower for  ${}^3\text{CDOM}^*$  ( $0.55\pm 0.05$ ) and direct photolysis ( $0.20\pm 0.02$ ). Conditions favouring  $\bullet\text{OH}$  reactivity would understandably enhance DEA formation. Among quantitatively less important intermediates, DEAOH and DIA are formed with similar yields upon direct photolysis and  $\bullet\text{OH}$  reaction, while CAAT and AN are formed by  ${}^3\text{CDOM}^*$ .
- DEA is unfortunately not a univocal marker of ATZ phototransformation (Mudhoo and Garg, 2011), despite its elevated formation yields. Indeed, ATZ biotic and abiotic transformation could not be easily distinguished by intermediate profiles. If sufficient information concerning photochemical parameters in the field is available, photochemical modelling could help assessing the relative role of photoinduced and biological processes. Important information about ATZ transformation pathways could also be derived from compound-specific isotope analysis (Hartenbach et al., 2008; Meyer et al., 2009).

#### *Acknowledgements*

Giulia Marchetti acknowledges a grant from the Lagrange Project – CRT Foundation. The authors are grateful to Riccardo Ariotti (owner of LAV s.r.l.) for co-financing the grant and for his support. Davide Vione acknowledges financial support from Università di Torino - EU Accelerating Grants, project TO\_Call2\_2012\_0047 (Impact of radiation on the dynamics of dissolved organic matter in aquatic ecosystems - DOMNAMICS).

## References

- Acero, J. L., Stemmler, K., Von Gunten, U., 2000. Degradation kinetics of atrazine and its degradation products with ozone and OH radicals: A predictive tool for drinking water treatment. *Environmental Science & Technology* 34, 591-597.
- Al Housari, F., Vione, D., Chiron, S., Barbati, S., 2010. Reactive photoinduced species in estuarine waters. Characterization of hydroxyl radical, singlet oxygen and dissolved organic matter triplet state in natural oxidation process. *Photochemical & Photobiological Sciences* 9, 78-86.
- Balci, B., Oturan, N., Cherrier, R., Oturan, M. A., 2009. Degradation of atrazine in aqueous medium by electrocatalytically generated hydroxyl radicals. A kinetic and mechanistic study. *Water Research* 43, 1924-1934.
- Bedini, A., De Laurentiis, E., Sur, B., Maurino, V., Minero, C., Brigante, M., Mailhot, G., Vione, D., 2012. Phototransformation of anthraquinone-2-sulphonate in aqueous solution. *Photochemical & Photobiological Sciences* 11, 1445-1453.
- Bhullar, M. S., Walia, U. S., Singh, S., Singh, M., Jhala, A. J., 2012. Control of Morningglories (*Ipomoea* spp.) in Sugarcane (*Saccharum* spp.). *Weed Technology* 26, 77-82.
- Bolton, J. R., Stefan, M. I., 2002. Fundamental photochemical approach to the concepts of fluence (UV dose) and electrical energy efficiency in photochemical degradation reactions. *Research on Chemical Intermediates* 28, 857-870.
- Bono-Blay, F., Guart, A., De la Fuente, B., Pedemonte, M., Pastor, M. C., Borrell, A., Lacorte, S., 2012. Survey of phthalates, alkylphenols, bisphenol A and herbicides in Spanish source waters intended for bottling. *Environmental Science & Pollution Research* 19, 3339-3349.
- Brassard, C., Gill, L., Stavola, A., Lin J., Turner, L., 2003. Atrazine Analysis of Risks. Endangered and Threatened Salmon and Steelhead Trout. US EPA Policy and Regulatory Services Branch and Environmental Field Branch, 25 pp.
- Buxton, G. V., Greenstock, C. L., Helman, W. P., Ross, A. B., 1988. Critical review of rate constants for reactions of hydrated electrons, hydrogen atoms and hydroxyl radicals ( $\cdot\text{OH}/\text{O}^{\cdot-}$ ) in aqueous solution. *Journal of Physical and Chemical Reference Data* 17, 513-886.
- Canonica, S., Kohn, T., Mac, M., Real, F. J., Wirz, J., Von Gunten, U., 2005. Photosensitizer method to determine rate constants for the reaction of carbonate radical with organic compounds. *Environmental Science & Technology* 39, 9182-9188.
- Canonica, S., Hellrung, B., Müller, P., Wirz, J., 2006. Aqueous oxidation of phenylurea herbicides by triplet aromatic ketones. *Environmental Science & Technology* 40, 6636-6641.
- Chung, S. W., Gu, R. R., 2009. Prediction of the fate and transport processes of atrazine in a reservoir. *Environmental Management* 44, 46-61.
- Cory, R. M., McKnight D. M., 2005. Fluorescence spectroscopy reveals ubiquitous presence of oxidized and reduced quinones in dissolved organic matter. *Environmental Science & Technology* 39, 8142-8149.



- De Laurentiis, E., Chiron, S., Kouras-Hadef, S., Richard, C., Minella, M., Maurino, V., Minero, C., Vione, D., 2012. Photochemical fate of carbamazepine in surface freshwaters: Laboratory measures and modeling. *Environmental Science & Technology* 46, 8164-8173.
- Fischer, M., Warneck, P., 1996. Photodecomposition of nitrite and undissociated nitrous acid in aqueous solution. *Journal of Physical Chemistry* 100, 18749-18756.
- Forgacs, A. L., Ding, Q., Jaremba, R. G., Huhtaniemi, I. T., Rahman, N. A., Zacharewski, T. R., 2012. BLTK1 murine Leydig cells: A novel steroidogenic model for evaluating the effects of reproductive and developmental toxicants. *Toxicological Sciences* 127, 391-402.
- Garbin, J. R., Milori, D. M. B. P., Simoes, M. L., Da Silva, W. T. L., Neto, L. M., 2007. Influence of humic substances on the photolysis of aqueous pesticide residues. *Chemosphere* 66, 1692-1698.
- Halladja, S., Ter Halle, A., Aguer, J. P., Boulkamh, A., Richard, C., 2007. Inhibition of humic substances mediated photooxygenation of furfuryl alcohol by 2,4,6-trimethylphenol. Evidence for reactivity of the phenol with humic triplet excited states. *Environmental Science & Technology* 41, 6066-6073.
- Hartenbach, A. E., Hofstetter, T. B., Tentscher, P. R., Canonica, S., Berg, M., Schwarzenbach, R. P., 2008. Carbon, hydrogen, and nitrogen isotope fractionation during light-induced transformations of atrazine. *Environmental Science & Technology* 42, 7751-7756.
- Huang, J., Mabury, S. A., 2000. A new method for measuring carbonate radical reactivity toward pesticides. *Environmental Toxicology and Chemistry* 19, 1501-1507.
- Kolpin, D. W., Kalkhoff, S. J., 1993. Atrazine degradation in a small stream in Iowa. *Environmental Science & Technology* 27, 134-139.
- Kuhn, H. J., Braslavsky, S. E., Schmidt, R., 2004. Chemical actinometry. *Pure and Applied Chemistry* 76, 2105-2146.
- Larson, R. A., Rupassara, S. I., Hothem, S. D., 2004. Green remediation of herbicides: Studies with atrazine. In: Nelson, W. M. (ed.), *Agricultural Applications in Green Chemistry*. ACS Symposium Series, Orlando, FL, vol. 887, pp. 129-139.
- Latch, D. E., Stender, B. L., Packer, J. L., Arnold, W. A., McNeill, K., 2003. Photochemical fate of pharmaceuticals in the environment: Cimetidine and ranitidine. *Environmental Science & Technology* 37, 3342-3350.
- Loeff, I., Treinin, A., Linschitz, H., 1983. Photochemistry of 9,10-anthraquinone-2-sulfonate in solution. 1. Intermediates and mechanism. *Journal of Physical Chemistry* 87, 2536-2544.
- Maddigapu, P. R., Bedini, A., Minero, C., Maurino, V., Vione, D., Brigante, M., Mailhot, G., Sarakha, M., 2010. The pH-dependent photochemistry of anthraquinone-2-sulfonate. *Photochemical & Photobiological Sciences* 9, 323-330.
- Maddigapu, P. R., Minella, M., Vione, D., Maurino, V., Minero, C., 2011. Modeling phototransformation reactions in surface water bodies: 2,4-Dichloro-6-nitrophenol as a case study. *Environmental Science & Technology* 45, 209-214.

- McConnell, L. L., Harman-Fetcho, J. A., Hagy, J. D., 2004. Measured concentrations of herbicides and model predictions of atrazine fate in the Patuxent river estuary. *Journal of Environmental Quality* 33, 594-604.
- Meyer, A. M., Penning, H., Elsner, M., 2009. C and N isotope fractionation suggests similar mechanisms of microbial atrazine transformation despite involvement of different enzymes (AtzA and TrzN). *Environmental Science & Technology* 43, 8079–8085.
- Minella, M., Rogora, M., Vione, D., Maurino, V., Minero, C., 2011. A model approach to assess the long-term trends of indirect photochemistry in lake water. The case of Lake Maggiore (NW Italy). *Science of the Total Environment* 409, 3463-3471.
- Minero, C., Pramauro, E., Pelizzetti, E., Dolci, M., Marchesini, A., 1992. Photosensitized transformation of atrazine under simulated sunlight in aqueous humic-acid solution. *Chemosphere* 24, 1597-1606.
- Mudhoo, A., Garg, V. K., 2011. Sorption, transport and transformation of atrazine in soils, minerals and composts: A review. *Pedosphere* 21, 11-25.
- Ou, X. X., Chen, S., Quan, X., Zhao, H. M., 2009. Photochemical activity and characterization of the complex of humic acids with iron(III). *J. Geochem. Explor.* 102, 49-55.
- Prosen, H., Zupančič-Kralj, L., 2005. Evaluation of photolysis and hydrolysis of atrazine and its first degradation products in the presence of humic acids. *Environmental Pollution* 133, 517-529.
- Reilly, T. J., Smalling, K. L., Orlando, J. L., Kuivila, K. M., 2012. Occurrence of boscalid and other selected fungicides in surface water and groundwater in three targeted use areas in the United States. *Chemosphere* 89, 228-234.
- Silva, E., Mendes, M. P., Ribeiro, L., Cerejeira, M. J., 2012. Exposure assessment of pesticides in a shallow groundwater of the Tagus vulnerable zone (Portugal): A multivariate statistical approach (JCA). *Environmental Science & Pollution Research* 19, 2667-2680.
- Sun, X., Liu, H., Zhang, Y. B., Zhao, Y. Z., Quan, X., 2011. Effects of Cu(II) and humic acid on atrazine photodegradation. *J. Environ. Sci.* 23, 773-777.
- Sur, B., De Laurentiis, E., Minella, M., Maurino, V., Minero, C., Vione, D., 2012. Photochemical transformation of anionic 2-nitro-4-chlorophenol in surface waters: Laboratory and model assessment of the degradation kinetics, and comparison with field data. *Science of the Total Environment* 426, 3197-3207.
- Takeda, K., Takedoi, H., Yamaji, S., Ohta, K., Sakugawa, H., 2004. Determination of hydroxyl radical photoproduction rates in natural waters. *Analytical Sciences* 20, 153-158.
- Tixier, C., Singer, H.P., Oellers, S., Müller, S.R., 2003. Occurrence and fate of carbamazepine, clofibric acid, diclofenac, ibuprofen, ketoprofen, and naproxen in surface waters. *Environmental Science & Technology* 37, 1061-1068.
- Torrents, A., Anderson, B. G., Bilbouljian, S., Johnson, W. E., Hapeman, C. J., 1997. Atrazine photolysis: Mechanistic investigations of direct and nitrate-mediated hydroxy radical processes

and the influence of dissolved organic carbon from the Chesapeake Bay. *Environmental Science & Technology* 31, 1476-1482.

US Environmental Protection Agency, 2012. Atrazine Updates (May 2012), [http://www.epa.gov/opp00001/reregistration/atrazine/atrazine\\_update.htm](http://www.epa.gov/opp00001/reregistration/atrazine/atrazine_update.htm), last accessed November 2012.

Vione, D., Khanra, S., Cucu Man, S., Maddigapu, P. R., Das, R., Arsene, C., Olariu, R. I., Maurino, V., Minero, C., 2009. Inhibition vs. enhancement of the nitrate-induced phototransformation of organic substrates by the  $\bullet\text{OH}$  scavengers bicarbonate and carbonate. *Water Research* 43, 4718-4728.

Vione, D., Das, R., Rubertelli, F., Maurino, V., Minero, C., Barbati, S., Chiron, S., 2010a. Modelling the occurrence and reactivity of hydroxyl radicals in surface waters: Implications for the fate of selected pesticides. *International Journal of Environmental Analytical Chemistry* 90, 258-273.

Vione, D., Khanra, S., Das, R., Minero, C., Maurino, V., Brigante, M., Mailhot, G., 2010b. Effect of dissolved organic compounds on the photodegradation of the herbicide MCPA in aqueous solution. *Water Research* 44, 6053-6062.

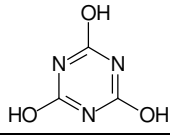
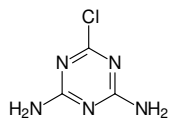
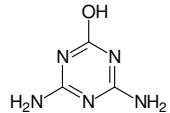
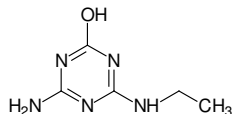
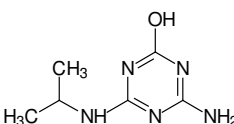
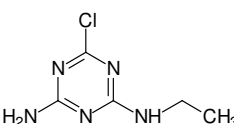
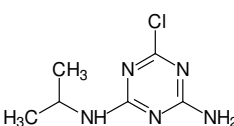
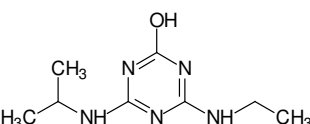
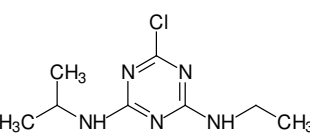
Vione, D., Maddigapu, P. R., De Laurentiis, E., Minella, M., Pazzi, M., Maurino, V., Minero, C., Kouras, S., Richard, C., 2011. Modelling the photochemical fate of ibuprofen in surface waters. *Water Research* 45, 6725-6736.

Wang, Q. F., Xie, S. G., 2012. Isolation and characterization of a high-efficiency soil atrazine-degrading *Arthrobacter* sp. strain. *International Biodeterioration & Biodegradation* 71, 61-66.

Warneck, P., Wurzinger, C., 1988. Product quantum yields from the 305-nm photodecomposition of  $\text{NO}_3^-$  in aqueous solution. *Journal of Physical Chemistry* 92, 6278-6283.

Zhang, Y., Meng, D. F., Wang, Z. G., Guo, H. S., Wang, Y., Wang, X., Dong, X. N., 2012. Oxidative stress response in atrazine-degrading bacteria exposed to atrazine. *Journal of Hazardous Materials* 229, 434-438.

**Table 1.** Structures, names, acronyms and chromatographic retention times ( $t_R$ ) of the studied compounds (ATZ and its potential or detected transformation intermediates). The transformation intermediates of ATZ that were detected and quantified are highlighted with a “☑”, those only detected but not quantified (too low concentration) with a “⊕”.

Molecule	Chemical (and common) name	Acronym	$t_R$ (min)
	2,4,6-Trihydroxy-1,3,5-triazine (cyanuric acid)	CYA ⊕	1.53
	2-Chloro-4,6-diamino-1,3,5-triazine	CAAT ☑	9.56
	2-Hydroxy-4,6-diamino-1,3,5-triazine (ammeline)	AN ☑	10.32
	6-Amino-4-ethylamino-2-hydroxy-1,3,5-triazine	DIAOH	13.71
	4-Amino-2-hydroxy-6-isopropylamino-1,3,5-triazine	DEAOH ☑	15.19 (*)
	6-Amino-2-chloro-4-ethylamino-1,3,5-triazine	DIA ☑	15.19 (*)
	4-Amino-2-chloro-6-isopropylamino-1,3,5-triazine	DEA ☑	17.08
	4-Ethylamino-2-hydroxy-6-isopropylamino-1,3,5-triazine	ATOH ⊕	18.88
	2-Chloro-4-ethylamino-6-isopropylamino-1,3,5-triazine (atrazine)	ATZ	21.17

(\*) DIA and DEAOH co-eluted, but it was possible to quantify both of them by exploiting the considerable differences in their absorption spectra. The relevant procedure is reported in the text.

**Table 2.** Photochemical parameters of ATZ degradation and intermediate formation *via* the different studied processes: UVB photolysis quantum yield of ATZ ( $\Phi$ , unitless) ( $^\circ$ ), second-order reaction rate constants with  $\bullet\text{OH}$ ,  $^3\text{CDOM}^*$ ,  $^1\text{O}_2$  and  $\text{CO}_3^{\bullet-}$  ( $k$ , units of  $\text{M}^{-1} \text{s}^{-1}$ ), and formation yields from ATZ of intermediates DEA, DEAOH, DIA, AN and CAAT ( $\eta$ , unitless).

	UVB photol.	$\bullet\text{OH}$	$^3\text{AQ2S}^*$	$^1\text{O}_2$	$\text{CO}_3^{\bullet-}$
ATZ, $\Phi$ or $k$	$(1.58 \pm 0.19) \cdot 10^{-2}$	$(2.7 \pm 0.3) \cdot 10^9$ (*)	$(1.43 \pm 0.07) \cdot 10^9$	$< 4 \cdot 10^4$	$4 \cdot 10^6$ (+)
DEA, $\eta$	$0.20 \pm 0.02$	$0.93 \pm 0.14$	$0.55 \pm 0.05$	Negligible	Negligible
DEAOH, $\eta$	$0.10 \pm 0.01$	$(8.6 \pm 4.6) \cdot 10^{-2}$	Negligible	Negligible	Negligible
DIA, $\eta$	$(8.5 \pm 1.1) \cdot 10^{-2}$	$(6.7 \pm 1.0) \cdot 10^{-2}$	Negligible	Negligible	Negligible
AN, $\eta$	Negligible	Negligible	$(2.3 \pm 0.8) \cdot 10^{-2}$	Negligible	Negligible
CAAT, $\eta$	Negligible	Negligible	$(2.3 \pm 0.9) \cdot 10^{-2}$	Negligible	Negligible

( $^\circ$ ) The UVB photolysis quantum yield of ATZ is applicable to environmental conditions, because ATZ absorbs sunlight only in the UVB region and only one band is involved in sunlight absorption.

(\*) Average of values reported by Acero et al. (2000) and Balci et al. (2009). All other values were determined in this work.

(+) This value has been determined by Huang and Mabury (2000).

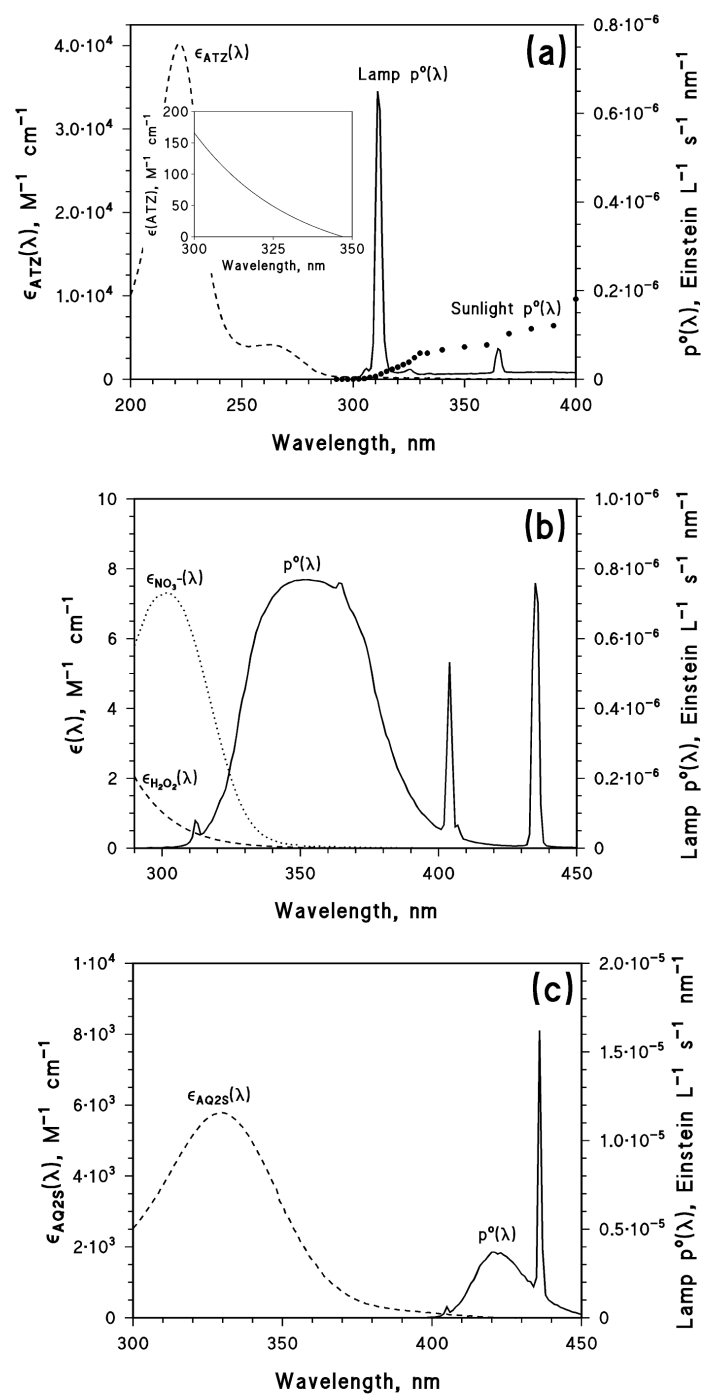


**Figure 1.** Absorption spectra (molar absorption coefficients) of: **(a)** ATZ (the insert shows its absorption spectrum above 300 nm); **(b)** nitrate and  $\text{H}_2\text{O}_2$ ; **(c)** AQ2S (anthraquinone-2-sulphonate). The spectral incident photon flux densities in solution of the lamps used to excite the relevant compounds are also reported: **(a)** TL 01 (emission maximum in the UVB region); **(b)** TL 09N (emission maximum in the UVA region); **(c)** TLK 03 (emission maximum in the blue region). Figure 1(a) also reports the absorption spectrum of sunlight that was used for photochemical modelling (see <http://chimica.campusnet.unito.it/do/didattica.pl/Quest?corso=7a3d>).

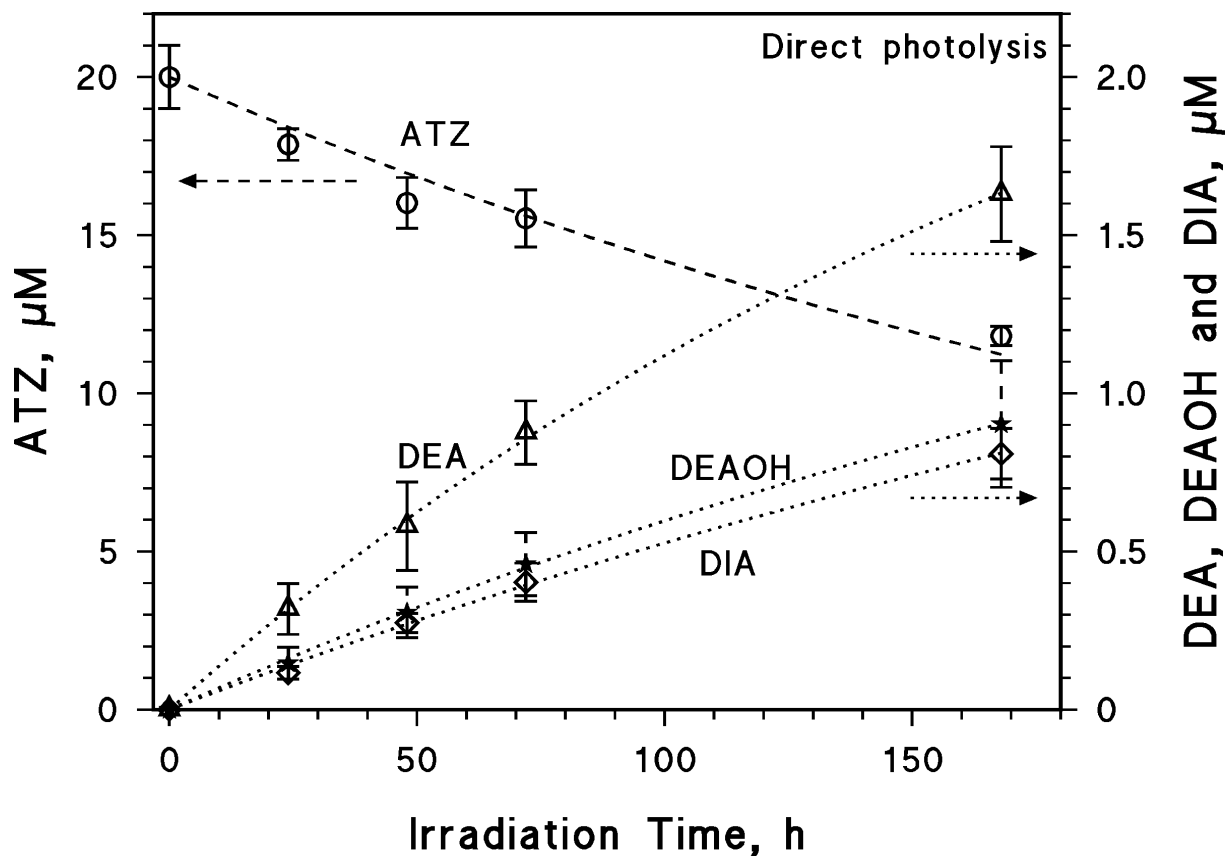


**Figure 2.** Time evolution of ATZ (initial concentration 20  $\mu\text{M}$ ) and of the intermediates DEA, DEAOH and DIA, upon irradiation under the TL 01 lamp (pH 6). Error bounds represent the standard deviation of replicate runs ( $\pm\sigma$ ).

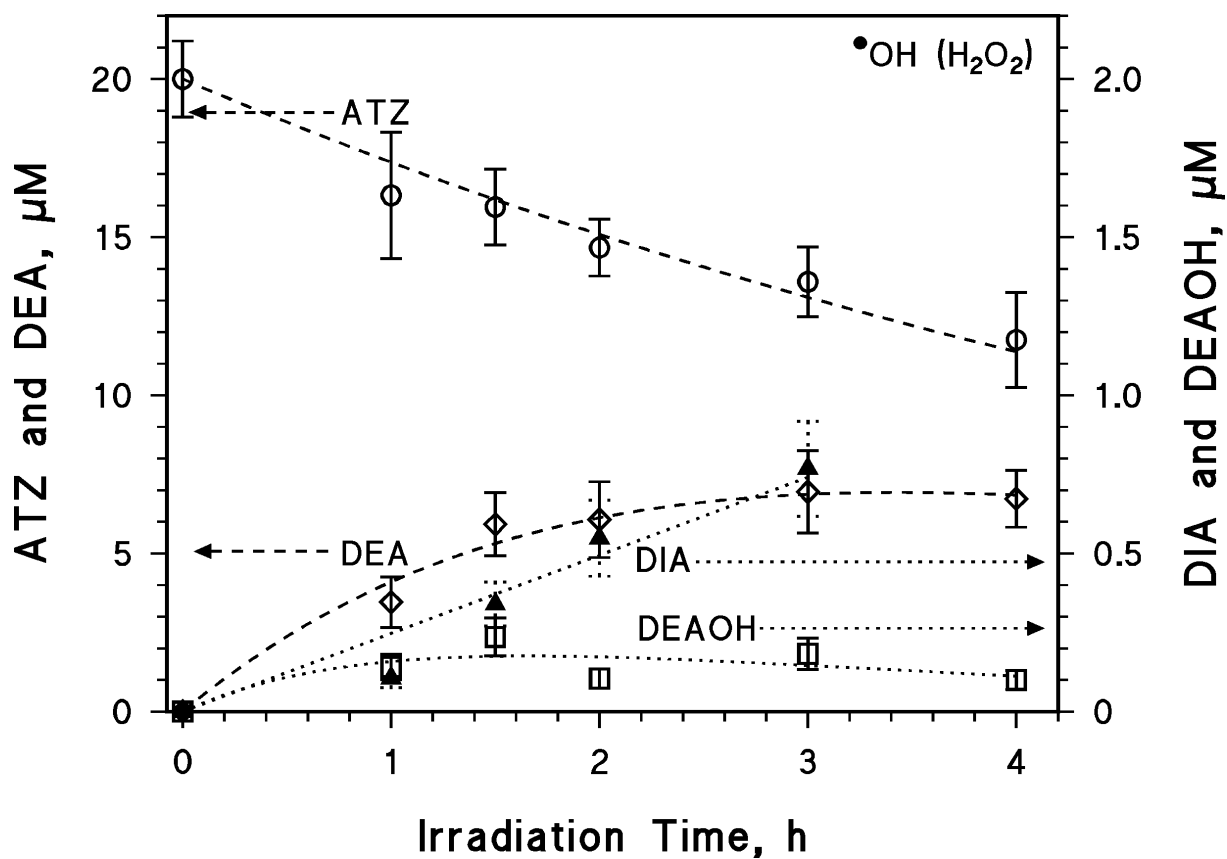


**Figure 3.** Time evolution of ATZ and the intermediates DEA, DEAOH and DIA upon irradiation of 20 μM ATZ and 1 mM H<sub>2</sub>O<sub>2</sub>, under the TL 09N lamp (pH 6). Note that ATZ and DEA on the one side, and DIA and DEAOH on the other are plotted versus different Y-axes. Error bounds represent the standard deviation of replicate runs ( $\pm\sigma$ ).



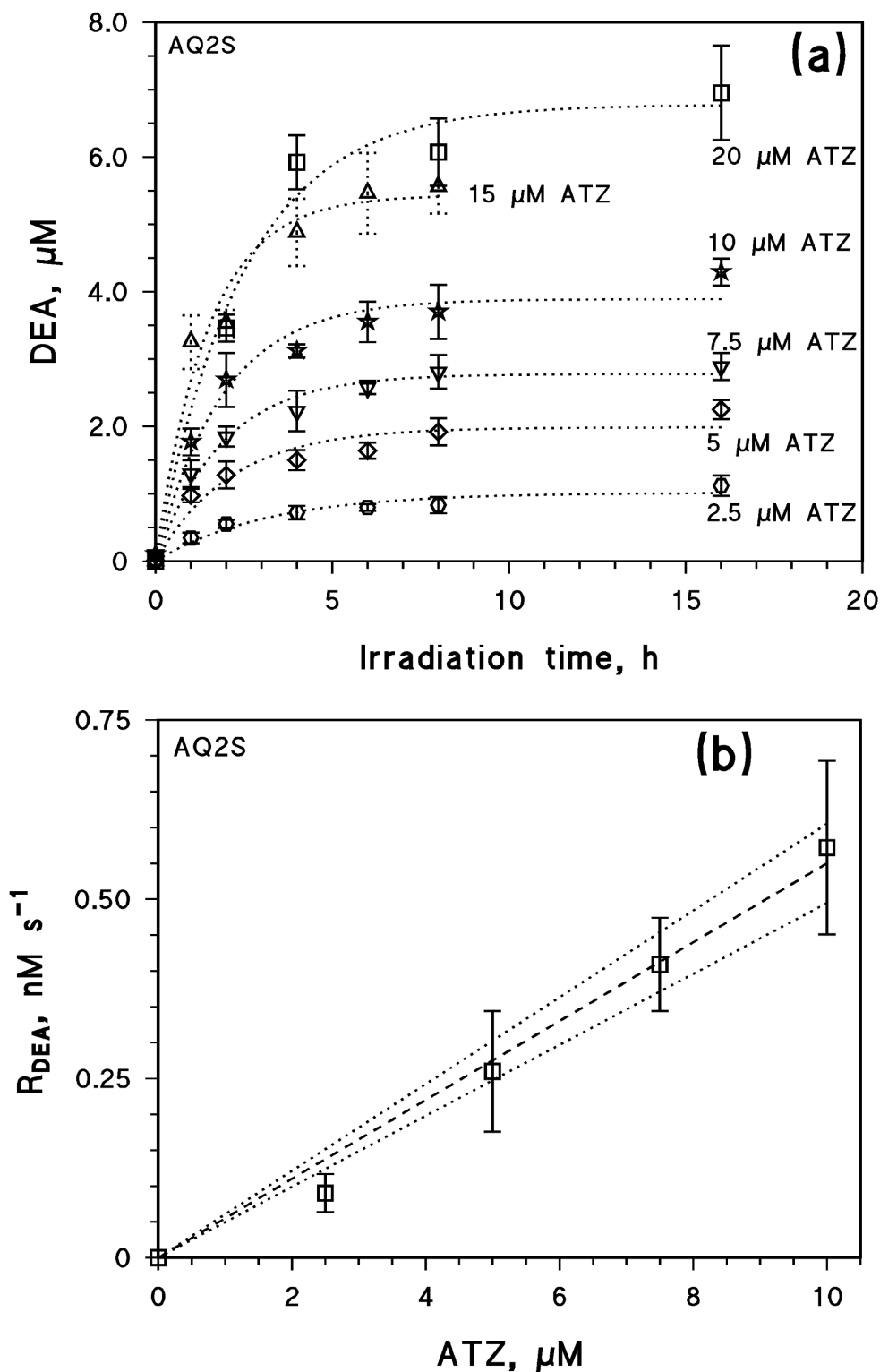


**Figure 4.** (a) Time evolution of DEA upon irradiation of 0.1 mM AQ2S in the presence of variable initial concentration values of ATZ, under the TLK 03 lamp (pH 6). Initial ATZ concentration values are reported near each data set. Error bounds represent the standard deviation of replicate runs ( $\pm\sigma$ ). (b) Initial formation rates of DEA as a function of ATZ initial concentration, under the same conditions.

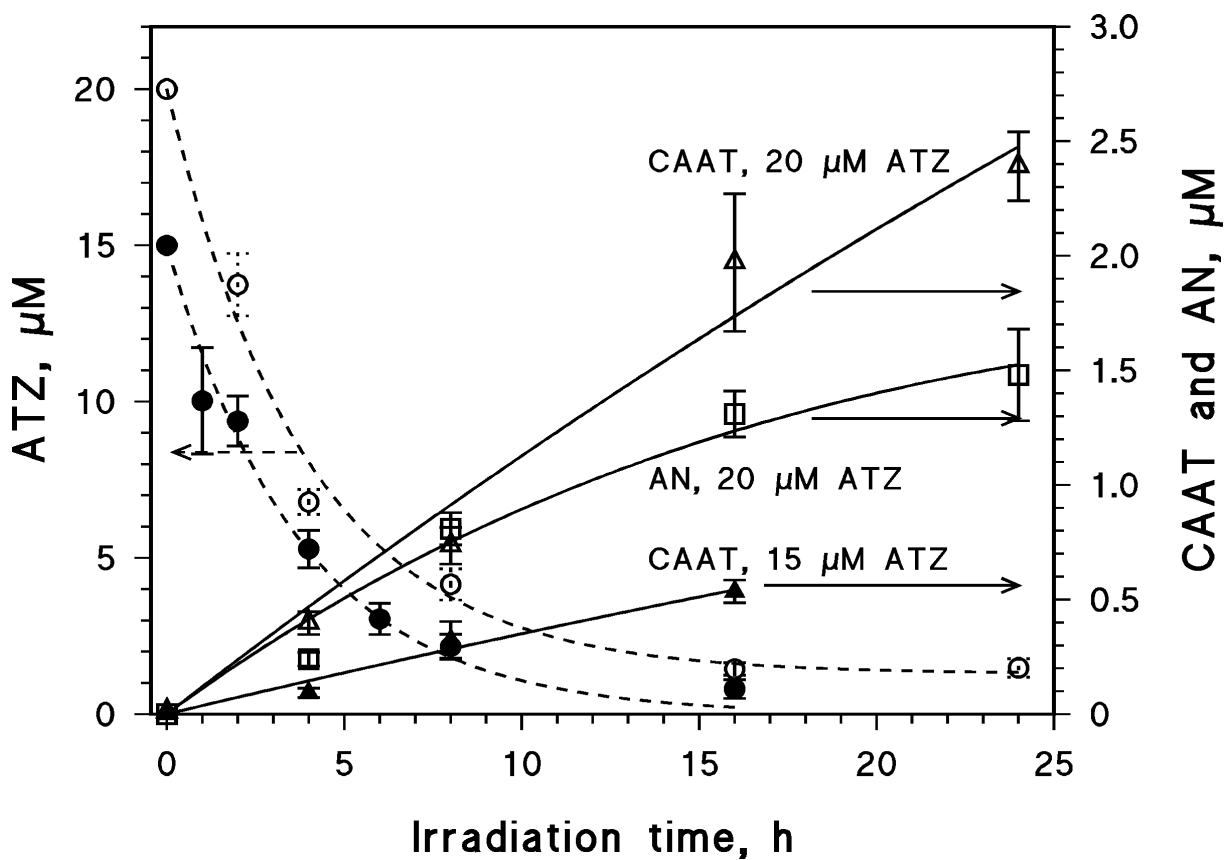


**Figure 5.** Time evolution of CAAT and AN upon irradiation of 0.1 mM AQ2S in the presence of 20  $\mu\text{M}$  (open symbols) and 15  $\mu\text{M}$  (solid symbols) initial ATZ, under the TLK 03 lamp (pH 6). The plot also reports the time evolution of 15 and 20  $\mu\text{M}$  ATZ. AN was below detection limit for 15  $\mu\text{M}$  ATZ. CAAT and AN were below detection limit for  $[\text{ATZ}]_0 < 15 \mu\text{M}$ . Error bounds represent the standard deviation of replicate runs ( $\pm\sigma$ ).

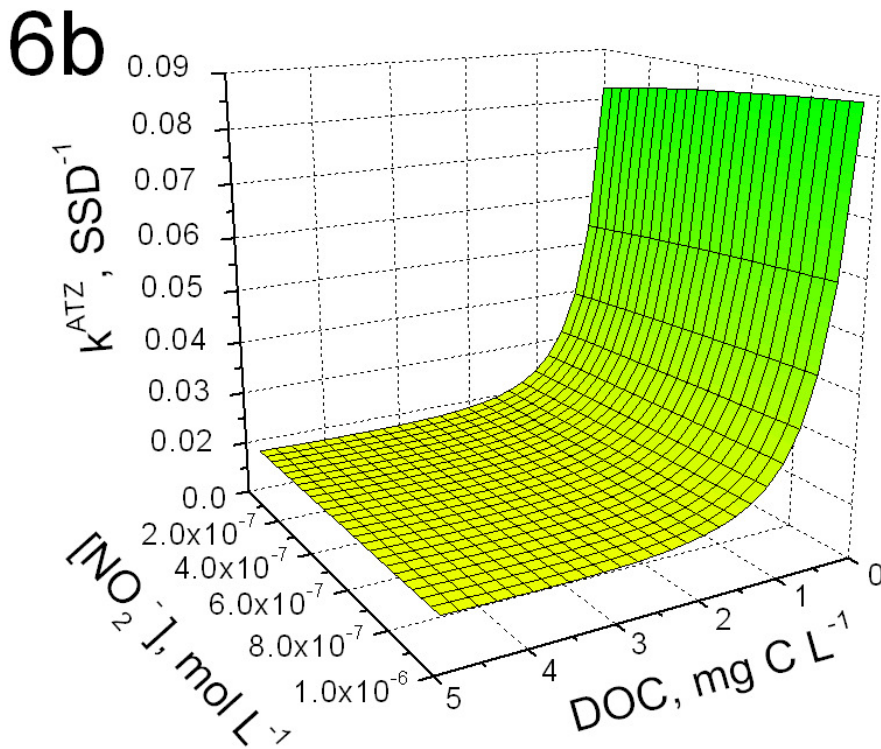
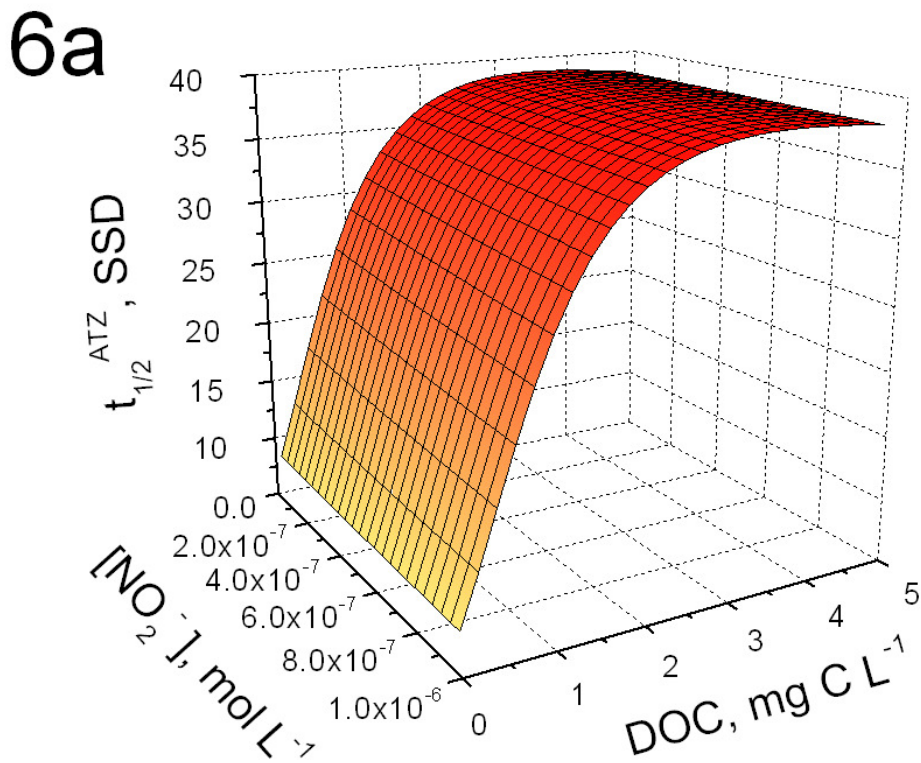


**Figure 6.** Modelled ATZ half-life time (a) and pseudo-first order degradation rate constant (b), as a function of nitrite and DOC. Other conditions: 5 m water depth, 50  $\mu$ M nitrate, 2 mM bicarbonate, 10  $\mu$ M carbonate.

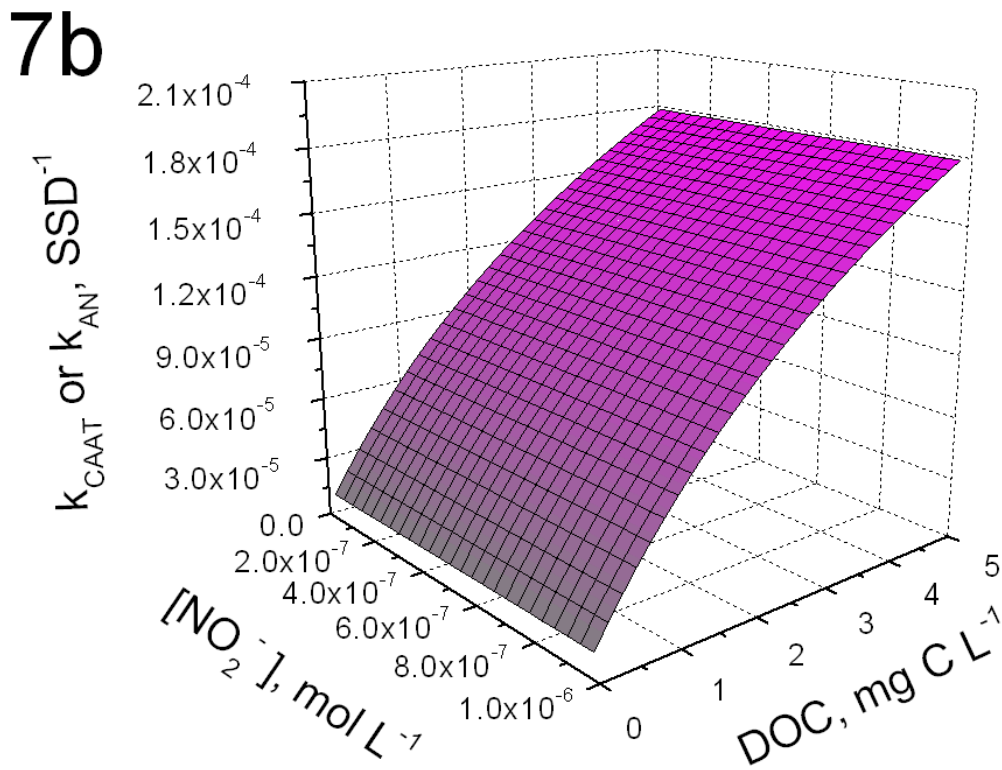
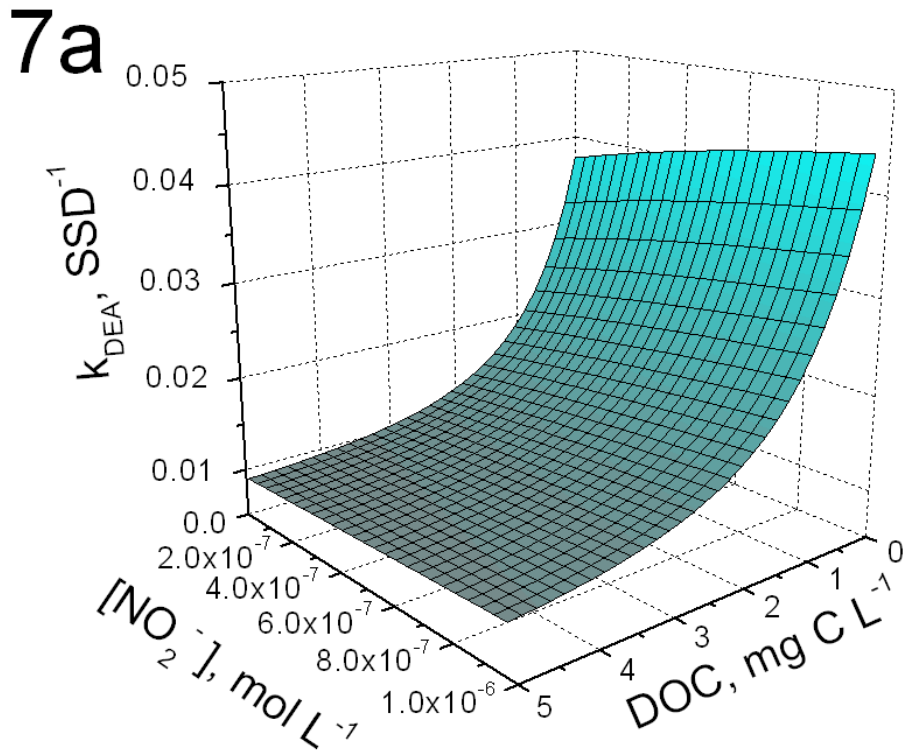


**Figure 7.** Pseudo-first order formation rate constants of: (a) DEA, (b) CAAT and AN, as a function of nitrite and DOC. Other conditions: 5 m water depth, 50  $\mu$ M nitrate, 2 mM bicarbonate, 10  $\mu$ M carbonate.

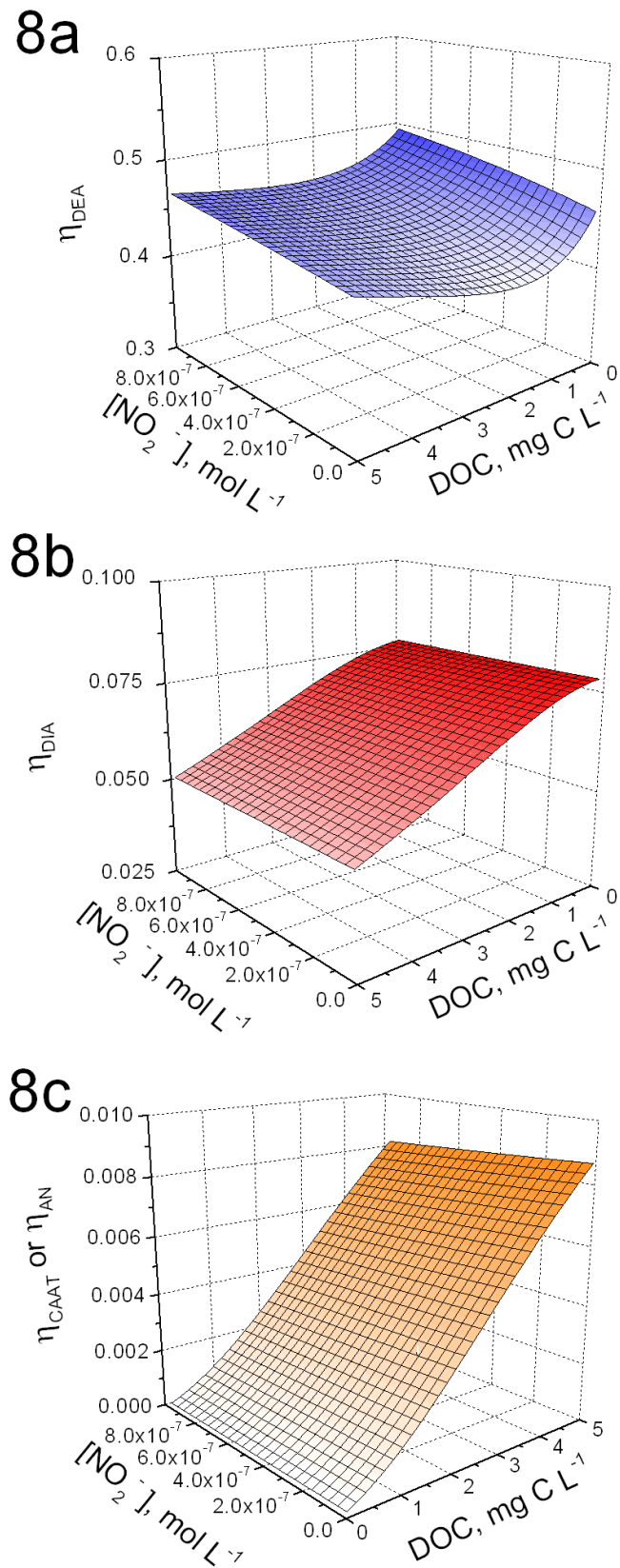


**Figure 8.** Formation yields from ATZ of: (a) DEA, (b) DIA, (c) CAAT and AN, as a function of nitrite and DOC. Other conditions: 5 m water depth, 50  $\mu\text{M}$  nitrate, 2 mM bicarbonate, 10  $\mu\text{M}$  carbonate.